Research Square

Preprints are preliminary reports that have not undergone peer review.
They should not be considered conclusive, used to inform clinical practice,
or referenced by the media as validated information.

Paternal folate deficiency induces hepatic insulin resistance in offspring mice

Jyotdeep Kaur

jyotdeep2001@yahoo.co.in

Post Graduate Institute of Medical Education and Research https://orcid.org/0000-0003-0284-4517

Parampal Singh

PGIMER

Divika Sapehia

PGIMER

Himanshi Goyal

PGIMER

Article

Keywords: folate deficiency, glucose tolerance, insulin resistance, metabolism, paternal nutrition

Posted Date: July 2nd, 2025

DOI: https://doi.org/10.21203/rs.3.rs-6543759/v1

License: This work is licensed under a Creative Commons Attribution 4.0 International License.
Read Full License

Additional Declarations: There is **NO** conflict of interest to disclose

Abstract

Background

Folate (vitamin B9) is a water-soluble vitamin necessary for one-carbon metabolism, supporting the synthesis, repair, and methylation of DNA. While maternal folate status is well-studied for its role in fetal development and metabolic programming, the impact of inadequate folate intake in males on offspring development and metabolic diseases remains poorly understood. This study investigates the effects of folate deficiency in male parents on developing hepatic insulin resistance in offspring, focusing on molecular and metabolic disruptions within the liver.

Methods

Three-week-old C57BL/6 male mice were categorized into two groups: Group I received a folate-normal (FN) diet, and Group II was fed a folate-deficient (FD) diet for four weeks before mating. F1 offspring from Group I (FN diet) were mated to produce F2 offspring (PNMN: paternal normal, maternal normal). F1 males from Group II (lifetime FD diet) were mated with F1 females on an FN diet to produce F2 offspring (PDMN: paternal deficient, maternal normal). F2 offspring from both groups were maintained on an FN diet and monitored for body weight. The study assessed systemic markers of insulin resistance, lipid and glucose metabolism, and gene expression profiles and proteins associated with insulin signaling in the liver. Mechanistic pathways involving lipid-induced and ER stress-triggered hepatic insulin resistance were explored.

Results

Male offspring born to folate-deficient fathers (PDMN) exhibited significantly elevated fasting glucose and insulin levels, impaired glucose tolerance, and increased insulin resistance indices (HOMA-IR, QUICKI) at 10 weeks. Hepatic insulin signaling was disrupted, as evidenced by downregulated p-AKT levels in 7-week PDMN males. Lipogenic pathways were upregulated, with increased expression of transcription factors *Srebf1c* and *Chrebp* (both at gene and protein levels), contributing to hepatic steatosis. Gluconeogenic genes, including *Foxo1*and *Fbp1*, were also upregulated, indicating elevated hepatic glucose output and exacerbation of hyperglycemia.

Chronic endoplasmic reticulum (ER) stress, marked by upregulation of *Perk* and *Atf6* (both at gene and protein levels), further impaired hepatic insulin signaling possibly by activating stress pathways and disrupting protein folding.

Conclusion

This study provides the first evidence that paternal folate deficiency predisposes offspring to hepatic insulin resistance by disrupting insulin signaling, promoting lipid dysregulation, and activating ER stress pathways. These effects are more severe in males, underscoring sex-specific susceptibility. The findings emphasize the importance of balanced paternal folate intake during reproduction to prevent intergenerational metabolic disorders and suggest potential therapeutic targets to mitigate hepatic insulin resistance caused by paternal nutritional deficiencies.

Introduction

Folate is a water-soluble vitamin that is crucial for DNA and RNA synthesis as well as amino acid metabolism. It is naturally found in dark green leafy vegetables, broccoli, peas and is also available as a dietary supplement. It functions as a coenzyme in single-carbon transfer reactions, crucial for nucleic acid synthesis and methylation processes. It is also essential for converting homocysteine to methionine, which subsequently aids in forming S-adenosylmethionine (SAM), a universal methyl group donor. This methylation process is vital for regulating phospholipids, proteins, DNA, and neurotransmitters. Given its role in epigenetic modifications, folate status has been implicated in influencing offspring health.

Maternal folate deficiency is well recognized for its association with neural tube defects (NTDs) in offspring (1). Recent research has further explored the metabolic consequences of maternal folate status. A study carried out in Pune, reported that elevated maternal folate levels combined with reduced vitamin B12 concentrations attributed to insulin resistance in offspring (2). An analysis of mother-child pairs in Boston found that maternal folate deficiency correlated with increased insulin levels and a reduced adiponectin-to-leptin ratio in offspring- biomarkers indicative of insulin resistance and sensitivity, respectively. Furthermore, maternal folate supplementation was found to mitigate the adverse metabolic effects associated with maternal obesity (3).

While the maternal influence of folate on offspring development is well studied, the role of paternal folate status remains relatively unexplored. However, emerging evidence suggests that paternal nutrition may significantly impact offspring health. Animal studies have demonstrated that paternal folate deficiency affects placental function and fetal development. For instance, Kim et al. observed that paternal folate-deficient rats exhibited reduced placental folate content and weight, along with an upregulation of folate receptor α (FRα), suggesting an adaptive response to maintain folate transport during pregnancy (4). Further investigations revealed that paternal folate deficiency was associated with increased congenital abnormalities, lower fetal liver folate levels, and impaired fetal brain development. Notably, even in the presence of normal maternal folate levels, paternal folate deficiency influenced fetal DNA methylation and altered insulin-like growth factor 2 (IGF-2) expression, suggesting an independent epigenetic effect of paternal folate status (5).

Additionally, folate status in males has been linked to sperm health and epigenetic modifications. Swayne et al. reported that male BALB/c mice subjected to a folate-deficient diet exhibited a 40% reduction in sperm count (6), whereas Lambrot et al. demonstrated significant changes in the sperm epigenome despite no alterations in sperm count (7). These epigenetic changes have been linked to a heightened susceptibility to metabolic diseases, such as cancer and diabetes. More recent studies in avian models have further supported the role of paternal folate in offspring metabolic health. Wu et al. reported that dietary folate supplementation in breeder cocks enhanced offspring growth and organ development, indicating a broader impact of paternal folate beyond mammalian models (8).

Despite growing evidence supporting the role of paternal folate in offspring development, studies investigating its effects on metabolic disorders remain scarce. Importantly, the influence of paternal folate insufficiency on insulin resistance in offspring remains to be explored. Using a murine model, this study aims to fill that gap by examining how paternal folate deficiency contributes to hepatic insulin resistance development in offspring. We hypothesize that paternal folate deficiency disrupts hepatic insulin signaling, leading to metabolic dysfunction in offspring. By elucidating these pathways, this research seeks to highlight the importance of paternal folate status in offspring metabolic health and provide strategies for mitigating the intergenerational effects of nutritional deficiencies.

Material and Methods

Animals

The study was approved by the Institute Animal Ethics Committee (763/IAEC/110). Three-week-old C57B/L6 male (n=8) and female mice (n=24) were procured from Advanced Small Animal Research Facility, PGIMER, Chandigarh, India. These were categorized into two groups; each one of the groups contained four male mice and twelve female mice and were fed commercial AIN-93G diets. In group I, both male and female mice were given a folic acid normal (FN) diet, and in group II, the mice received a folic acid deficient (FD) diet for four weeks before mating (Fig. 1).

Mating was confirmed in females from both groups by tracing a vaginal plug, denoted as day 0, and pregnant mice were housed individually. The offspring of both groups were named as the F1 generation. F1 mice from group I continued the FN diet and were mated, the offspring (F2) were named PNMN (paternal normal maternal normal). After weaning from FD mothers, F1 males from group II continued the folic acid deficient diet (lifetime deficient male mice) and were mated with F1 females having a lifetime folic acid normal diet. F2 offspring from this group were weaned on an FN diet and were designated as PDMN (paternal deficient maternal normal). F2 offspring were allowed to grow further, and body weight was examined throughout the experimental phase twice a week. F2 mice were sacrificed at weeks seven and ten, and further experiments were performed on male and female offspring separately.

G**lucose tolerance test (GTT) and Insulin tolerance test (ITT)**

Animals were subjected to fasting for 6h, and blood glucose levels were assessed before injecting glucose or insulin for GTT and ITT, respectively. In the case of GTT, 1.5g of glucose/kg body mass was injected intraperitoneally while 0.75 IU insulin/kg body mass was administered intraperitoneally for performing ITT. Glucose measurements were made at 15 min, 30 min, 60 min, and 90 min using Roche Accu-Chek Active Glucometer. Area under the curve (AUC) was analyzed using GraphPad prism.

Measurement of insulin levels

Blood was collected from the hepatic portal vein after the sacrifice of animals and was left to clot for half an hour. The serum collection was done after centrifugation at 1000 x g at 4°C for 10 minutes. Insulin levels were measured in serum using Mouse Insulin High Sensitivity ELISA, BioVendor Research and Diagnostic Products (Brno, Czech Republic). Experiment was carried out using the kit manual and absorbance was recorded at 450 nm, and concentration was determined using a standard curve.

HOMA-IR, HOMA-B, and QUICKI

i) Homeostatic model assessment for insulin resistance (HOMA - IR) is an index for assessing the degree of insulin resistance and was determined using the following formula (9):

HOMA-IR= fasting insulin (μU/mL) × fasting glucose (mmol/L)/22.5

ii) Homeostatic model assessment for beta cell function (HOMA-B) is an index of insulin secretory function and was calculated using the formula (10):

HOMA-B= (20 × insulin in μU/mL)/(glucose in mmol/L - 3.5)

iii) QUICKI (Quantitative Insulin Sensitivity Check Index) is an index to assess insulin sensitivity and was calculated using the formula (11):

QUICKI = (1/log insulin (μU/mL) + log glucose (mg/dL))

Biochemical Analysis

Serum folate levels were assessed using the electrochemiluminescence method on the Cobas ECLIA e 411 analyzer (Roche Diagnostics GmbH, Mannheim, Germany). Liver function tests, lipid profile, and hepatic triglyceride levels were studied using the Beckman Coulter AU5800 analyzer**.**

mRNA expression studies

Total RNA was isolated from liver tissues adopting TRIzol method (Thermo Fisher Scientific, USA). Complementary DNA (cDNA) was synthesized utilizing iScript Reverse Transcription Supermix (Bio-Rad, USA), with 1 μg of total RNA in a 20 μL reaction mixture. Quantitative real-time PCR (qRT-PCR) was performed using SYBR® Green chemistry on the Bio-Rad CFX96 Real-Time PCR System. Primers targeting genes related to insulin signaling, lipid metabolism, and ER stress, including *Insr*, *Irs1*, *Irs2*, *Akt*, *Gsk3β*, *Foxo1*, *Srebf1c*, *Chrebp*, *Fbp1*, *Perk*, and *Atf6*, were designed using Primer-BLAST (NCBI) and validated for specificity and efficiency. Gene expression patterns were corrected against *β-actin*, and the fold change was determined with $2^{-\Delta\Delta CT}$ method.

Protein expression analysis

Liver tissues were lysed in RIPA buffer. The concentration of isolated proteins was quantified by utilizing the bicinchoninic acid (BCA) assay (Thermo Fisher Scientific, USA). Protein was loaded in equal

amounts, separated electrophoretically through SDS-PAGE, and subsequently blotted onto polyvinylidene fluoride (PVDF) membranes. Blocking of the membrane was done using skimmed milk or 5% BSA and incubated with primary antibodies specific to AKT, p-AKT, (Cell Signaling Technology, USA), SREBP, CHREBP, (Affinity Biosciences, USA), ATF6, (Abclonal, USA), and β-ACTIN (Cell Signaling Technology, USA). The membranes were incubated with an HRP-conjugated goat anti-rabbit IgG secondary antibody (Cell Signaling Technology, USA), and protein signals were visualized with the Western Blotting Substrate Clarity Max ECL (Bio-Rad, USA), and band intensity was quantified using ImageJ software.

Immunohistochemistry (IHC)

Liver tissues were stabilized in 10% neutral buffered formalin, immobilized within paraffin, and sliced into sections 3-5 µm thick. Tissue microarrays (TMAs) were constructed using 2 mm core punches from representative regions, with each TMA block containing duplicate samples from the PNMN and PDMN groups. Tissue sections were deparaffinized, rehydrated, and underwent antigen retrieval using citrate buffer (pH 6.0). To inhibit endogenous peroxidase activity, 3% hydrogen peroxide was applied. Sections were incubated with primary antibodies against SREBP, FOXO1, ATF6, and PERK (1:200 dilution) in a humidified chamber at room temperature for 1.5 hours, followed by incubation with HRP-conjugated antibodies. DAB substrate was used for signal visualization and Hematoxylin was applied for contrast staining of the sections. Slides were mounted with DPX and examined under a light microscope.

Statistical evaluation

Statistical assessment was done using GraphPad Prism 8 and Excel 2019. Results are expressed as mean ± standard deviation (SD). Control and test group comparisons were done using unpaired Student's t-test, while non-parametric test-Mann-Whitney U test, was applied to validate the findings. A p-value of ≤ 0.05 indicates statistical significance.

Results

Paternal folate deficiency impacts circulatory markers and lipid profiles in offspring

The influence of reduced paternal folate levels on body weight, serum folate levels, and lipid profiles was measured in F2 offspring. No marked difference in the body weight was observed between PDMN (paternal deficient, maternal normal) and PNMN (paternal normal, maternal normal) groups in both males and females across 7 and 10 weeks, though a slight upward trend in body weight was noted in 10-week-old mice (Supplementary fig. 1A-D).

Biochemical analysis revealed elevated LDL levels in 7-week-old PDMN males (1.5-fold, $p<0.05$) and females (1.7-fold, $p<0.05$), indicating early lipid metabolism disruption (Table 1 in supplementary data). At 10 weeks, ALT levels were notably enhanced in PDMN males (1.8-fold, $p<0.05$), while ALP levels were elevated in PDMN females (1.8-fold, $p<0.05$) (Table 2 in supplementary data). These findings suggest subtle liver function impairments and lipid dysregulation associated with paternal folate deficiency.

Elevated hepatic triglycerides

Triglyceride (TG) accumulation, a marker of metabolic dysregulation, was measured in liver tissue. Liver TG amounts were markedly elevated in both sexes in PDMN mice at both 7 weeks (2.0-fold, $p<0.01$) and 10 weeks (1.4-fold, $p<0.01$) (Supplementary fig. 1E, F).

Paternal folate deficiency induces hyperinsulinemia, and hyperglycemia in male offspring

To explore glucose metabolism, fasting insulin and glucose, and postprandial glucose levels were determined. Fasting insulin levels were significantly increased in 10-week PDMN males (99.5%, $p<0.05$) (Fig. 2a, b). Fasting glucose levels were similarly elevated in 10-week PDMN mice, with a significant increase in both males (38.2%, $p<0.05$) and females (26.5%, $p<0.05$) (Fig. 2c, d).

Postprandial glucose levels mirrored fasting glucose trends, with a 43.7% increase in PDMN 10-week males ($p<0.05$), while females remained unaffected (Fig. 2e, f). These findings suggest that paternal folate deficiency contributes to hyperinsulinemia and impaired glucose metabolism, particularly in male offspring.

Impaired GTT and ITT in male offspring of folate-deficient fathers

GTT and ITT were performed to evaluate glucose homeostasis. At 10 weeks, PDMN males exhibited significant glucose intolerance, with a 118% increase in the area under the curve (AUC) during GTT ($p<0.05$), while females showed no significant changes (Fig. 3a, b). Similarly, insulin tolerance was impaired in 10-week PDMN males, with a 15.8% increase in AUC during ITT ($p<0.05$), but no differences were noted in females (Fig. 3c, d). These results highlight a sex-specific susceptibility to impaired glucose and insulin tolerance due to paternal folate deficiency.

Paternal folate deficiency increases insulin resistance markers without affecting beta-cell function

To further investigate impaired insulin sensitivity, HOMA-B (beta-cell function), HOMA-IR (insulin resistance), and QUICKI (insulin sensitivity) indices were calculated. At 10 weeks, HOMA-IR values were notably elevated in PDMN male mice, with a 123% increase ($p<0.05$) relative to the PNMN group (Fig. 3e, f). In contrast, HOMA-B values remained unchanged across groups (Supplementary fig. 1g, h), indicating preserved beta-cell function. QUICKI values decreased significantly at 10 weeks in PDMN male mice (9.6%, $p<0.05$) indicating reduced insulin sensitivity (Fig. 3g, h). These findings suggest that paternal folate deficiency promotes insulin resistance, primarily in male offspring, without compromising beta-cell function.

Effect of paternal folate deficiency on various genes involved in insulin signaling and lipid metabolism

The insulin receptor encoding gene *Insr*, showed a significant increase in 7-week-old PDMN males (1.95-fold, $p<0.05$) and 10-week-old PDMN females (2.27-fold, $p<0.05$) compared to PNMN controls (Fig. 4a, b). Similarly, *Irs1* expression was significantly upregulated in female PDMN mice at both 7 weeks (2.2-

fold, $p < 0.05$) and 10 weeks (6.4-fold, $p < 0.01$), while males exhibited no significant changes (Fig. 4c, d). Similarly, *Irs2* expression showed a notable increase in both male (3.8-fold, $p < 0.01$) and female (3.2-fold, $p < 0.05$) PDMN mice at 7 weeks, but no significant alterations were observed in either sex at 10 weeks (Fig. 4e, f). *Akt*, a central mediator of insulin action, exhibited increased expression in both sexes, with a more pronounced elevation in males at 7 weeks (4.1-fold, $p<0.001$) and sustained upregulation at 10 weeks (1.8-fold, $p<0.05$) (Fig. 4g, h). *Gsk3β* expression, was significantly increased in both sexes. At 7 weeks, males and females exhibited 2.3-fold ($p<0.05$) and 1.6-fold ($p<0.05$) increases, respectively. This increase was also observed at 10 weeks, with males showing a 1.5-fold increase ($p<0.05$) and females a 2.3-fold increase ($p<0.05$), suggesting potential disruptions in glycogen synthesis contributing to altered glucose metabolism (Fig. 4i, j). *Fbp1* expression was elevated in both sexes, but the response was more pronounced in males (3.0-fold, $p<0.05$) (Fig. 4k, l)

Foxo1 expression was significantly increased in PDMN males at 7 weeks (3.1-fold, $p<0.05$), with no considerable changes in females at this time point. By 10 weeks, *Foxo1* was elevated in both males (2.2-fold, $p<0.05$) and females (5.0-fold, $p<0.01$), (Fig. 4m, n). *Srebf1c* and *Chrebp* were significantly upregulated in PDMN males at both 7 and 10 weeks ($p<0.05$), while females exhibited no significant changes (Fig. 4o-r).

Effect of paternal folate deficiency on various proteins involved in insulin signaling and lipid metabolism

Despite the transcriptional upregulation of *Akt*, immunoblot analysis revealed a pronounced reduction in phosphorylated AKT (p-AKT) levels in 7-week PDMN males (1.4-fold decrease, $p<0.05$), suggesting impaired insulin signaling downstream of receptor activation. No notable differences were identified in females (Fig. 5a, d, and e).

Further, a notable increase in SREBP protein levels in PDMN males at 10 weeks (5.2-fold, $p<0.05$) and in females (2.2-fold, $p<0.05$) (Fig. 5b, f, and g) was observed. Similarly, CHREBP protein levels were notably augmented in PDMN males at both 7 weeks (1.5-fold, $p<0.05$) and 10 weeks (1.7-fold, $p<0.05$), while females showed no considerable alterations (Fig. 5c, h and i).

Immunohistochemical analysis:

IHC analysis corroborated the molecular findings, showing increased nuclear FOXO expression in PDMN liver tissues, particularly in males (Fig. 6A-D, I). Similarly, SREBP expression demonstrated increased nucleo-cytoplasmic localization in PDMN males as compared to PNMN controls. Females also showed moderate upregulation but to a lesser extent (Fig. 6E-H, J).

Effect of paternal folate deficiency on ER stress-induced hepatic insulin resistance

To assess the involvement of ER stress in impaired hepatic insulin signaling, the gene and protein expression of key markers of ER stress was evaluated. At the gene level, Perk was significantly upregulated in PDMN males at 7 weeks (9.3-fold, $p<0.01$), while females showed a moderate

upregulation (4.3-fold, $p<0.05$) (Fig. 7a). At 10 weeks, both sexes showed increased Perk expression, with males showing a 3.2-fold increase ($p<0.05$) and females a 4.6-fold increase ($p<0.05$) (Fig. 7b). Western blot analysis confirmed these findings, with phosphorylated PERK (p-PERK) levels significantly elevated in 10 week PDMN males (5.5-fold, $p<0.05$) and females (3.3-fold, $p<0.05$) (Fig. 7e-h). These findings were further supported by IHC analysis, which revealed increased cytoplasmic localization of PERK and p-PERK in PDMN liver tissues (Fig. 8A-H, M, and N).

Similarly, Atf6 expression was significantly elevated in PDMN females both at 7 weeks (2.4-fold, $p<0.01$) and 10 weeks (2.5-fold, $p<0.01$) while male PDMN mice exhibited a notable increase only at 10 weeks (1.7-fold, $p<0.05$) (Fig. 7c, d). ATF6 protein expression on the other hand was significantly upregulated in PDMN males at both 7 weeks (1.6-fold, $p<0.05$) and 10 weeks (1.8-fold, $p<0.05$), while females exhibited no significant changes (Fig. 7f-j). Further, IHC analysis of ATF6 showed increased nucleo-cytoplasmic staining in PDMN mice (Fig. 8I-L, O), highlighting enhanced ER stress signaling in response to paternal folate deficiency.

Discussion

This study investigated the effects of paternal folate deficiency on offspring metabolic health, focusing on insulin sensitivity and liver function. Our findings provide novel evidence that even when mothers receive normal folate, paternal folate deficiency can program hepatic insulin resistance in the offspring. Notably, these metabolic disturbances are largely sex-specific, with male offspring exhibiting greater susceptibility to insulin resistance and hepatic dysfunction than females. These results extend the DOHaD (developmental origins of health and disease) concept to paternal nutrition, emphasizing that a father's dietary status at conception can have long-lasting consequences on progeny (12).

Circulatory markers of insulin resistance and sex-specific effects

Fasting glucose and insulin levels, along with glucose and insulin tolerance tests, revealed that by 10 weeks of age, male offspring of folate-deficient fathers displayed markedly elevated fasting insulin and glucose levels, as well as impaired glucose tolerance. The increased HOMA-IR and decreased QUICKI in PDMN males quantitatively confirm reduced insulin sensitivity. Importantly, these changes emerged despite the offspring being maintained on a folate-sufficient diet postnatally, indicating that the paternal factors programmed the risk. . In contrast, female offspring showed only modest increases in fasting glucose, with largely normal insulin and glucose tolerance tests, suggesting a protective effect possibly mediated by estrogen and other sex hormones that enhance insulin sensitivity and lipid metabolism (13).

Moreover, despite similar growth trajectories and body weights between PDMN and PNMN groups, metabolic dysfunction manifested as ectopic fat accumulation and dyslipidemia in the PDMN group. Early increases in LDL cholesterol in both male and female PDMN offspring at 7 weeks point to a predisposition for dyslipidemia-a risk factor for insulin resistance and cardiovascular disease (14). By 10 weeks, subtle elevations in liver enzymes (ALT in males, ALP in females) indicated hepatic stress. Given

that folate is essential for homocysteine metabolism and its deficiency may impair lipid handling (15, 16), these findings suggest that paternal folate deficiency imposes metabolic strain on the liver and circulation independent of overall adiposity.

Hepatic insulin signaling and glucose metabolism mechanisms

At the molecular level, paternal folate deficiency induced significant alterations in hepatic insulin signaling pathways. We observed upregulation of *Insr*, *Irs1*, *Irs2*, and *Akt2* transcripts in PDMN livers (particularly at 7 weeks), likely reflecting a compensatory response to early insulin resistance (17, 18). Such upregulation might enhance the capacity of hepatocytes to capture insulin when circulating levels are high; indeed, *Irs1* was notably increased in PDMN females, perhaps contributing to their relatively preserved insulin signaling compared to males.

Despite these transcriptional adaptations, there was a ~40% reduction in phosphorylated AKT in PDMN males, indicating a post-receptor defect in insulin signaling. Since AKT2 is critical for promoting glucose uptake and suppressing hepatic gluconeogenesis, its reduced activation suggests the presence of inhibitory factors such as serine phosphorylation of IRS proteins, lipid intermediates, or stress kinase activation (19). This impairment aligns with classic models of insulin resistance, wherein partial attenuation of insulin signaling leads to hyperglycemia (20, 21).

Upregulation of *Foxo1* and *Fbp1* in PDMN livers further explains the hyperglycemia observed. Normally, insulin-mediated AKT activation inhibits FOXO1, thereby suppressing gluconeogenesis. In PDMN males, elevated *Foxo1* expression and nuclear FOXO1 localization indicate that insulin fails to restrain gluconeogenic gene expression, resulting in increased hepatic glucose output. This finding is concordant with Zhang et al., who demonstrated that suppression of Foxo1 and Foxo3 reduces hyperglycemia and hyperlipidemia, thereby confirming that elevated FOXO1 is a critical determinant of hepatic gluconeogenesis (22). In our study, the persistent upregulation of Foxo1 suggests a failure of insulin to adequately inactivate this pathway in PDMN males.

Additionally, persistent upregulation of *Gsk3β* would impair glycogen synthesis and promote gluconeogenesis, further exacerbating hyperglycemia. Patel et al. showed that GSK3β plays major role in glucose homeostasis and its overactivity is linked to impaired insulin action (23). Cline et al. further illustrated that inhibition of GSK3 improves insulin signaling (24), supporting our observation that elevated Gsk3β in PDMN livers contributes to the hyperglycemic phenotype.

Hepatic lipid metabolism dysregulation

Our findings also reveal disrupted lipid metabolism in the offspring of folate-deficient fathers. Despite normal chow feeding, PDMN male offspring exhibited elevated hepatic triglycerides. This was accompanied by upregulation of key lipogenic transcription factors, SREBP-1c and ChREBP, at both the mRNA and protein levels. Although insulin is a primary inducer of SREBP-1c, hyperinsulinemia in PDMN males may sustain its activation even as other insulin signaling pathways are not functional. This

“selective insulin resistance” leads to persistent lipogenesis alongside impaired suppression of gluconeogenesis which has been observed in other models. Linden et al. demonstrated that coordinated activation of ChREBP and SREBP-1c is crucial for postprandial lipogenesis, confirming that elevated SREBP-1c in our model supports sustained lipogenesis (25). Ruiz et al. also emphasized the role of SREBP-1 in regulating both glycogen synthesis and gluconeogenesis (26), while Denechaud et al. linked ChREBP activation with hepatic steatosis, further corroborating our interpretation of selective insulin resistance (27).

Further, there was increased expression of ChREBP in PDMN males which might be resulting in an anabolic drive within hepatocytes and subsequent triglyceride accumulation. Moreover, folate deficiency can disrupt the production of SAM, which is critical for phosphatidylcholine synthesis and VLDL export; impaired export may further contribute to fat accumulation in the liver (16). Our observations are consistent with previous reports showing paternal B vitamin intake influences hepatic lipid metabolism (28).

ER stress and its role in insulin resistance

A critical finding is the induction of chronic ER stress in the livers of offspring from folate-deficient fathers. We observed robust activation of the PERK and ATF6 branches of the unfolded protein response (UPR) in PDMN mice. PERK phosphorylation, which normally attenuates protein synthesis and induces stress response genes, was significantly elevated in PDMN livers, suggesting that chronic PERK activation contributes to insulin resistance by impairing insulin signal transduction and promoting gluconeogenesis. These results are supported by Zhang et al. who reported that folate deficiency in male mice leads to PERK-mediated ER stress, linking compromised one-carbon metabolism to defects in insulin signaling (29). Fang et al. further showed that targeting PERK can alleviate fatty acid–induced insulin resistance, suggesting that elevated PERK in our study not only serves as a marker of ER stress but also actively disrupts insulin signaling (30). Lee et al.’s findings on partial PERK deletion improving glucose tolerance reinforce the idea that chronic PERK activation is detrimental to glucose homeostasis, aligning well with our observations (31).

ATF6, which translocates to the nucleus to upregulate ER chaperones and degradation machinery, display a dual role. While acute ATF6 activation is adaptive, chronic activation may lead to lipid dysregulation and inflammation. Chen et al. reported that liver-specific activation of ATF6 increased fatty acid oxidation and mitigated steatosis, suggesting that short-term ATF6 activation can be beneficial (32). However, our model indicates that persistent ATF6 activation, as seen in PDMN males, likely reflects an insufficient compensatory response, thereby contributing to steatosis and insulin resistance. Cinaroglu et al. demonstrated that chronic ATF6 activation can have pathological outcomes in the context of steatosis (33). Thus, while ATF6’s initial role may be protective, its sustained activation in our study suggests that it eventually contributes to the metabolic dysfunction observed in PDMN offspring. Chronic ER stress may also exacerbate insulin resistance by activating JNK, which phosphorylates IRS-1 and further impairs insulin signaling (19).

Potential epigenetic mechanisms and intergenerational implications

Although our study did not directly measure epigenetic modifications, the data strongly imply that epigenetic mechanisms mediate the transmission of metabolic abnormalities from folate-deficient fathers to their offspring. Folate's central role in the one-carbon cycle is critical for DNA methylation, and paternal folate deficiency likely alters the sperm methylome. Previous studies have documented that low paternal folate results in differential DNA methylation in sperm and altered expression of imprinted genes in offspring (7). Moreover, paternal folate deficiency has been linked to changes in imprinting control regions and gene expression, suggesting that promoters of key metabolic genes could exhibit impaired methylation (34). Altered sperm microRNA content in folate-deficient males could also contribute to these intergenerational effects.

Our study shows that, despite overall insulin resistance, lipogenesis remains intact in the offspring. This selective insulin resistance is similar to what is observed in the offspring of fathers fed a high-fat diet where sperm epigenetic changes drive the metabolic phenotype (35, 36). These findings suggest that paternal folate deficiency can also program metabolic disorders in offspring, expanding the concept of intergenerational programming to include micronutrient status.

From a public health perspective, these findings underscore the importance of considering paternal folate status in reproductive planning. In populations where men may have suboptimal folate intake due to dietary limitations or malabsorptive conditions, there may be unrecognized consequences for the metabolic health of their children (37). Ensuring optimal paternal folate intake prior to conception may represent a simple, cost-effective strategy to mitigate the risk of intergenerational metabolic disorders.

Conclusion

In summary, our study demonstrates for the first time that paternal folate deficiency can program hepatic insulin resistance in offspring in a sex-dependent manner. The male-biased metabolic dysfunction is characterized by impaired insulin signaling (reduced p-AKT), enhanced gluconeogenesis (increased FOXO1 and FBP1), upregulated GSK3β, and dysregulated lipogenesis (increased SREBP-1c and ChREBP), compounded by chronic ER stress. These findings not only extend our understanding of intergenerational metabolic programming but also highlight the critical role of paternal nutrition. Future studies should explore the reversibility of these programmed changes and delineate the underlying epigenetic modifications involved, thereby informing nutritional guidelines for prospective fathers to improve offspring metabolic health.

Abbreviations

AUC: Area under curve

GTT: Glucose tolerance test

ITT: Insulin tolerance test

HOMA-IR: Homeostasis model assessment of insulin resistance

HOMA-B: Homeostasis model assessment of β-cell function

NTD: Neural tube defects

QUICKI: Quantitative insulin sensitivity check index

SAM: S-Adenosyl methionine

Declarations

Declaration of Interests

The authors declare that they have no conflicts of interest.

Author Contributions

Mr. Parampal Singh performed the experiments, analyzed the data, and drafted the manuscript. **Dr. Divika Sapehia** and **Ms. Himanshi Goyal** assisted with animal work, biochemical assays, and data collection. **Prof. Jyotdeep Kaur** designed the research study and provided overall supervision. She critically revised the manuscript for important intellectual content. All authors have read and approved the final version of the manuscript.

Acknowledgements

This work was supported by DBT sponsored project (BT/PR41478/MED/97/511/2020). We would also like to acknowledge Council of Scientific and Industrial Research, India for fellowship to Parampal Singh (09/141(0215)/2019-EMR-I).

References

1. Greenberg JA, Bell SJ, Guan Y, Yu YH. Folic Acid supplementation and pregnancy: more than just neural tube defect prevention. Rev Obstet Gynecol. 2011;4(2):52-9.
2. Yajnik CS, Deshpande SS, Jackson AA, Refsum H, Rao S, Fisher DJ, et al. Vitamin B12 and folate concentrations during pregnancy and insulin resistance in the offspring: the Pune Maternal Nutrition Study. Diabetologia. 2008;51(1):29-38.
3. Wang G, Hu FB, Mistry KB, Zhang C, Ren F, Huo Y, et al. Association Between Maternal Prepregnancy Body Mass Index and Plasma Folate Concentrations With Child Metabolic Health. JAMA Pediatr. 2016;170(8):e160845.

4. Kim HW, Choi YJ, Kim KN, Tamura T, Chang N. Effect of paternal folate deficiency on placental folate content and folate receptor alpha expression in rats. Nutr Res Pract. 2011;5(2):112-6.
5. Kim HW, Kim KN, Choi YJ, Chang N. Effects of paternal folate deficiency on the expression of insulin-like growth factor-2 and global DNA methylation in the fetal brain. Mol Nutr Food Res. 2013;57(4):671-6.
6. Swayne BG, Kawata A, Behan NA, Williams A, Wade MG, Macfarlane AJ, et al. Investigating the effects of dietary folic acid on sperm count, DNA damage and mutation in Balb/c mice. Mutat Res. 2012;737(1-2):1-7.
7. Lambrot R, Xu C, Saint-Phar S, Chountalos G, Cohen T, Paquet M, et al. Low paternal dietary folate alters the mouse sperm epigenome and is associated with negative pregnancy outcomes. Nat Commun. 2013;4:2889.
8. Wu S, Guo W, Li X, Liu Y, Li Y, Lei X, et al. Paternal chronic folate supplementation induced the transgenerational inheritance of acquired developmental and metabolic changes in chickens. Proc Biol Sci. 2019;286(1910):20191653.
9. Matthews DR, Hosker JP, Rudenski AS, Naylor BA, Treacher DF, Turner RC. Homeostasis model assessment: insulin resistance and beta-cell function from fasting plasma glucose and insulin concentrations in man. Diabetologia. 1985;28(7):412-9.
10. Wei S, Han R, Zhao J, Wang S, Huang M, Wang Y, et al. Intermittent administration of a fasting-mimicking diet intervenes in diabetes progression, restores beta cells and reconstructs gut microbiota in mice. Nutr Metab (Lond). 2018;15:80.
11. Katz A, Nambi SS, Mather K, Baron AD, Follmann DA, Sullivan G, et al. Quantitative insulin sensitivity check index: a simple, accurate method for assessing insulin sensitivity in humans. J Clin Endocrinol Metab. 2000;85(7):2402-10.
12. Shi Q, Qi K. Developmental origins of health and disease: Impact of paternal nutrition and lifestyle. Pediatr Investig. 2023;7(2):111-31.
13. Mauvais-Jarvis F. Sex differences in metabolic homeostasis, diabetes, and obesity. Biol Sex Differ. 2015;6:14.
14. Paredes S, Fonseca L, Ribeiro L, Ramos H, Oliveira JC, Palma I. Novel and traditional lipid profiles in Metabolic Syndrome reveal a high atherogenicity. Sci Rep. 2019;9(1):11792.
15. Yang M, Wang D, Wang X, Mei J, Gong Q. Role of Folate in Liver Diseases. Nutrients. 2024;16(12).
16. da Silva RP, Kelly KB, Al Rajabi A, Jacobs RL. Novel insights on interactions between folate and lipid metabolism. Biofactors. 2014;40(3):277-83.
17. Hennige AM, Burks DJ, Ozcan U, Kulkarni RN, Ye J, Park S, et al. Upregulation of insulin receptor substrate-2 in pancreatic beta cells prevents diabetes. J Clin Invest. 2003;112(10):1521-32.
18. Galicia-Garcia U, Benito-Vicente A, Jebari S, Larrea-Sebal A, Siddiqi H, Uribe KB, et al. Pathophysiology of Type 2 Diabetes Mellitus. Int J Mol Sci. 2020;21(17).

19. Khalid M, Alkaabi J, Khan MAB, Adem A. Insulin Signal Transduction Perturbations in Insulin Resistance. Int J Mol Sci. 2021;22(16).
20. Lu M, Wan M, Leavens KF, Chu Q, Monks BR, Fernandez S, et al. Insulin regulates liver metabolism in vivo in the absence of hepatic Akt and Foxo1. Nat Med. 2012;18(3):388-95.
21. Cho H, Mu J, Kim JK, Thorvaldsen JL, Chu Q, Crenshaw EB, 3rd, et al. Insulin resistance and a diabetes mellitus-like syndrome in mice lacking the protein kinase Akt2 (PKB beta). Science. 2001;292(5522):1728-31.
22. Zhang K, Li L, Qi Y, Zhu X, Gan B, DePinho RA, et al. Hepatic suppression of Foxo1 and Foxo3 causes hypoglycemia and hyperlipidemia in mice. Endocrinology. 2012;153(2):631-46.
23. Patel S, Doble BW, MacAulay K, Sinclair EM, Drucker DJ, Woodgett JR. Tissue-specific role of glycogen synthase kinase 3beta in glucose homeostasis and insulin action. Mol Cell Biol. 2008;28(20):6314-28.
24. Cline GW, Johnson K, Regittnig W, Perret P, Tozzo E, Xiao L, et al. Effects of a novel glycogen synthase kinase-3 inhibitor on insulin-stimulated glucose metabolism in Zucker diabetic fatty (fa/fa) rats. Diabetes. 2002;51(10):2903-10.
25. Linden AG, Li S, Choi HY, Fang F, Fukasawa M, Uyeda K, et al. Interplay between ChREBP and SREBP-1c coordinates postprandial glycolysis and lipogenesis in livers of mice. J Lipid Res. 2018;59(3):475-87.
26. Ruiz R, Jideonwo V, Ahn M, Surendran S, Tagliabracci VS, Hou Y, et al. Sterol regulatory element-binding protein-1 (SREBP-1) is required to regulate glycogen synthesis and gluconeogenic gene expression in mouse liver. J Biol Chem. 2014;289(9):5510-7.
27. Denechaud PD, Dentin R, Girard J, Postic C. Role of ChREBP in hepatic steatosis and insulin resistance. FEBS Lett. 2008;582(1):68-73.
28. Sabet JA, Park LK, Iyer LK, Tai AK, Koh GY, Pfalzer AC, et al. Paternal B Vitamin Intake Is a Determinant of Growth, Hepatic Lipid Metabolism and Intestinal Tumor Volume in Female Apc1638N Mouse Offspring. PLoS One. 2016;11(3):e0151579.
29. Zhang Y, Yuan H, Peng M, Hu Z, Fan Z, Xu J, et al. Folic acid deficiency damages male reproduction via endoplasmic reticulum stress-associated PERK pathway induced by Caveolin-1 in mice. Syst Biol Reprod Med. 2021;67(5):383-94.
30. Fang Z, Gao W, Jiang Q, Loor JJ, Zhao C, Du X, et al. Targeting IRE1alpha and PERK in the endoplasmic reticulum stress pathway attenuates fatty acid-induced insulin resistance in bovine hepatocytes. J Dairy Sci. 2022;105(8):6895-908.
31. Lee J, Kim MJ, Moon S, Lim JY, Park KS, Jung HS. Partial Deletion of Perk Improved High-Fat Diet-Induced Glucose Intolerance in Mice. Endocrinol Metab (Seoul). 2023;38(6):782-7.
32. Chen X, Zhang F, Gong Q, Cui A, Zhuo S, Hu Z, et al. Hepatic ATF6 Increases Fatty Acid Oxidation to Attenuate Hepatic Steatosis in Mice Through Peroxisome Proliferator-Activated Receptor alpha. Diabetes. 2016;65(7):1904-15.

33. Cinaroglu A, Gao C, Imrie D, Sadler KC. Activating transcription factor 6 plays protective and pathological roles in steatosis due to endoplasmic reticulum stress in zebrafish. Hepatology. 2011;54(2):495-508.
34. Ly L, Chan D, Aarabi M, Landry M, Behan NA, MacFarlane AJ, et al. Intergenerational impact of paternal lifetime exposures to both folic acid deficiency and supplementation on reproductive outcomes and imprinted gene methylation. Mol Hum Reprod. 2017;23(7):461-77.
35. de Castro Barbosa T, Ingerslev LR, Alm PS, Versteyhe S, Massart J, Rasmussen M, et al. High-fat diet reprograms the epigenome of rat spermatozoa and transgenerationally affects metabolism of the offspring. Mol Metab. 2016;5(3):184-97.
36. Crean AJ, Senior AM, Freire T, Clark TD, Mackay F, Austin G, et al. Paternal dietary macronutrient balance and energy intake drive metabolic and behavioral differences among offspring. Nat Commun. 2024;15(1):2982.
37. Khan KM, Jialal I. Folic Acid Deficiency. StatPearls. Treasure Island (FL)2025.

Tables

Table 1. Biochemical parameters (liver function test, lipid profile, and folate levels) studied in the serum of 7 week males and females. *p<0.05 vs. PNMN control.

Parameters	7-week males		7-week females	
	PNMN	PDMN	PNMN	PDMN
Albumin (g/dL)	2.96±0.63	3.19±0.19	3.11±0.58	3.99±0.29*
Alkaline phosphatase (U/L)	141.70±20.21	108.30±12.58	145.00±33.42	121.30±21.36
Alanine aminotransferase (U/L)	28.67±9.08	29.67±4.54	46.50±9.88	51.43±7.62
Aspartate aminotransferase (U/L)	92.33±35.20	88.67±31.15	110.10±16.78	96.25±35.91
Total cholesterol (mg/dL)	122.90±19.35	146.00±19.17	112.30±23.15	119.90±7.56
HDL (mg/dL)	91.63±14.45	101.40±12.09	83.63±21.90	80.50±7.31
LDL (mg/dL)	15.50±2.18	23.50±5.00*	11.17±0.76	19.17±2.36*
Total protein (g/dL)	5.46±0.89	5.44±0.54	5.08±0.52	5.87±0.31
Triglyceride (mg/dL)	170.60±14.44	145.80±18.48	154.40±20.23	154.40±46.42
Folate (ng/mL)	68.16±8.45	74.70±16.20	84.68±13.06	67.08±6.84

Table 2. Biochemical parameters (liver function test, lipid profile, and folate levels) were studied in the serum of 10-week males and females. *p<0.05 vs. PNMN control.

Parameters	10 week males		10 week females	
	PNMN	PDMN	PNMN	PDMN
Albumin (g/dL)	3.31±0.21	3.41±0.10	3.90±0.25	3.70±0.33
Alkaline phosphatase (U/L)	100.00±8.66	81.67±14.43	67.50±20.62	121.30±29.26*
Alanine aminotransferase (U/L)	18.33±7.64	33.13±2.84*	25.17±3.21	20.17±2.36
Aspartate aminotransferase (U/L)	72.50±23.60	92.25±41.08	70.10±10.04	62.33±16.26
Total cholesterol (mg/dL)	150.90±12.74	165.50±12.06	116.00±12.53	126.00±2.56
HDL (mg/dL)	109.20±3.64	108.80±5.51	81.17±4.37	79.17±20.10
LDL (mg/dL)	19.33±2.52	18.67±0.76	16.33±1.15	15.50±2.00
Total protein (g/dL)	5.91±0.62	5.50±0.29	5.87±0.57	5.38±0.39
Triglyceride (mg/dL)	157.00±18.70	166.50±12.29	164.70±23.69	133.80±26.50
Folate (ng/mL)	72.63±8.94	61.63±12.91	68.93±3.74	68.03±5.32

Figures

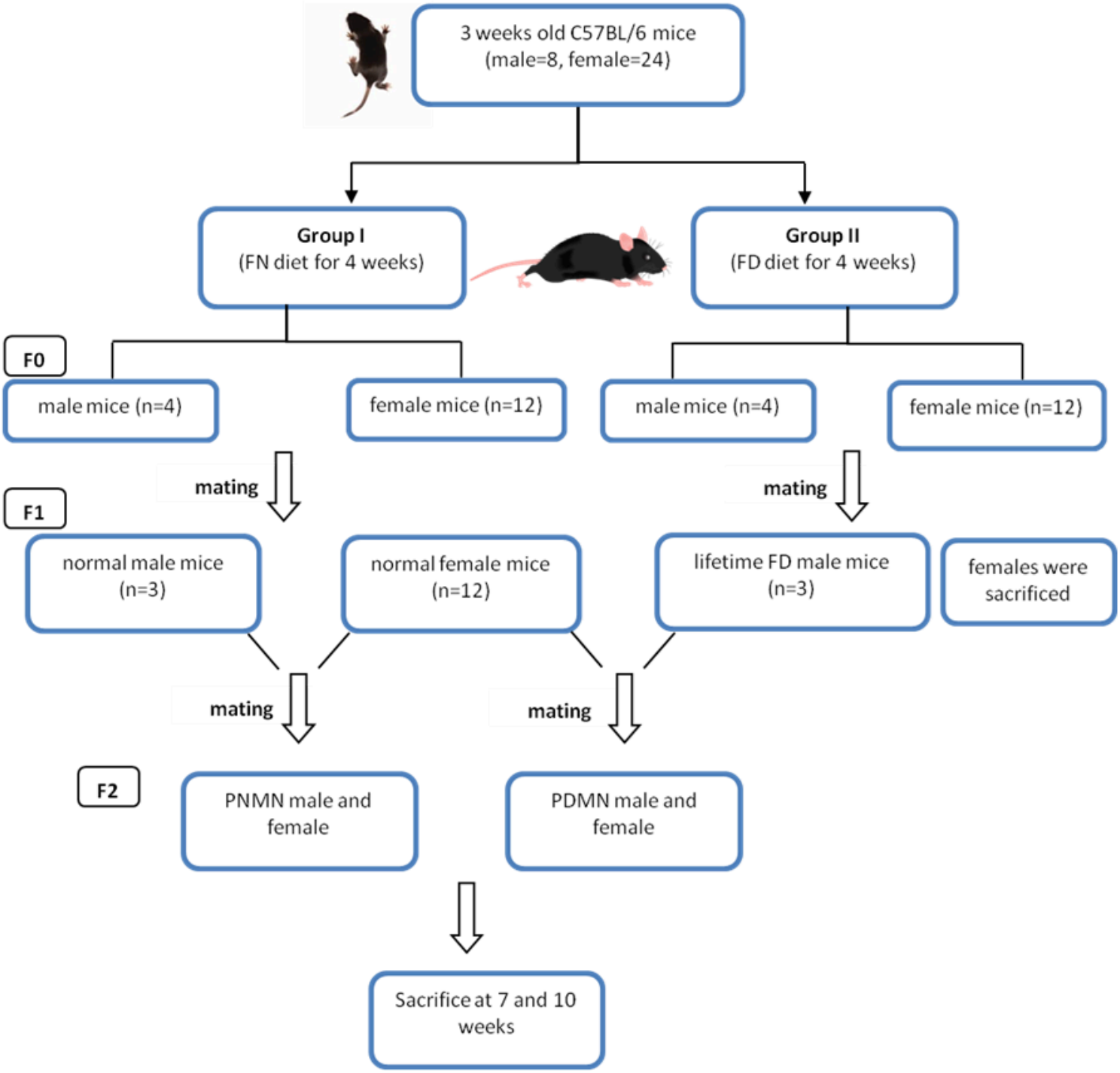


Figure 1

Experimental design of the paternal folate-deficiency model. Three-week-old C57BL/6 males (n=8) and females (n=24) were fed either a folate-normal (FN, Group I) or folate-deficient (FD, Group II) diet for 4 weeks. F0 males from Group I and Group II were mated with FN females to generate F1 offspring. F1 males from the FN lineage (PNMN) and FD lineage (PDMN) were then mated with FN females to produce the F2 generation. F2 pups were maintained on FN diet and sacrificed at 7 and 10 weeks for metabolic and molecular analyses. FN: Folate normal diet (2mg/kg body weight), FD:Folate deficient diet (0mg/kg

body weight + 1% succinyl-sulfathiazole), PNMN: Paternal Normal Maternal Normal, PDMN: Paternal Deficient Maternal Normal.

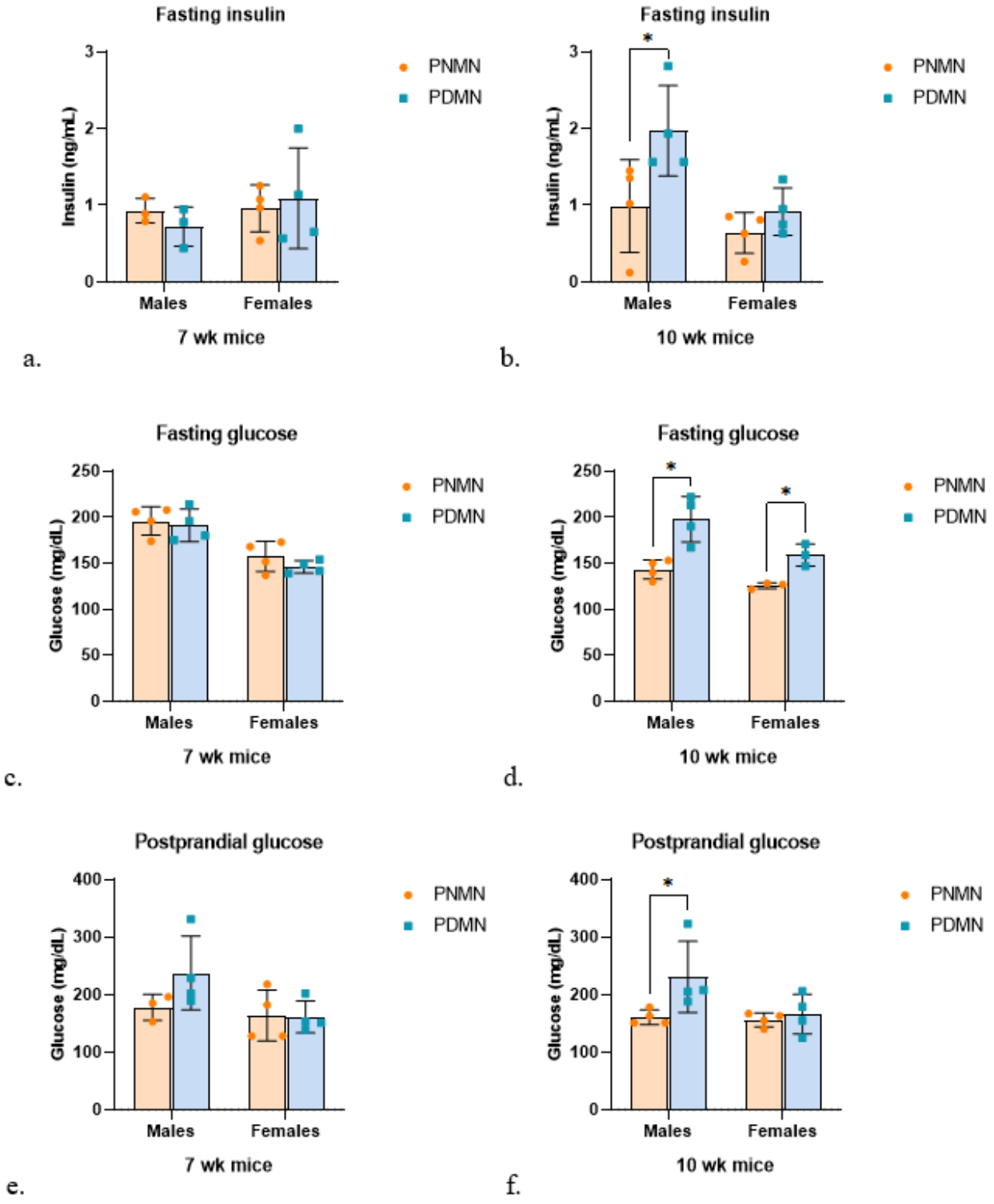


Figure 2

Paternal folate deficiency elevates fasting and postprandial glucose and insulin in F2 offspring. Fasting serum insulin in (a) 7-week mice and in (b) 10-week males. Fasting blood glucose in (c) 7-week mice and

in (d) 10-week mice. Postprandial blood glucose in (e) 7-week mice and in (f) 10-week mice. Data is represented as mean ± SD; PNMN-Paternal normal maternal normal diets, PDMN-Paternal deficient maternal normal diets. *p<0.05 vs. PNMN control.

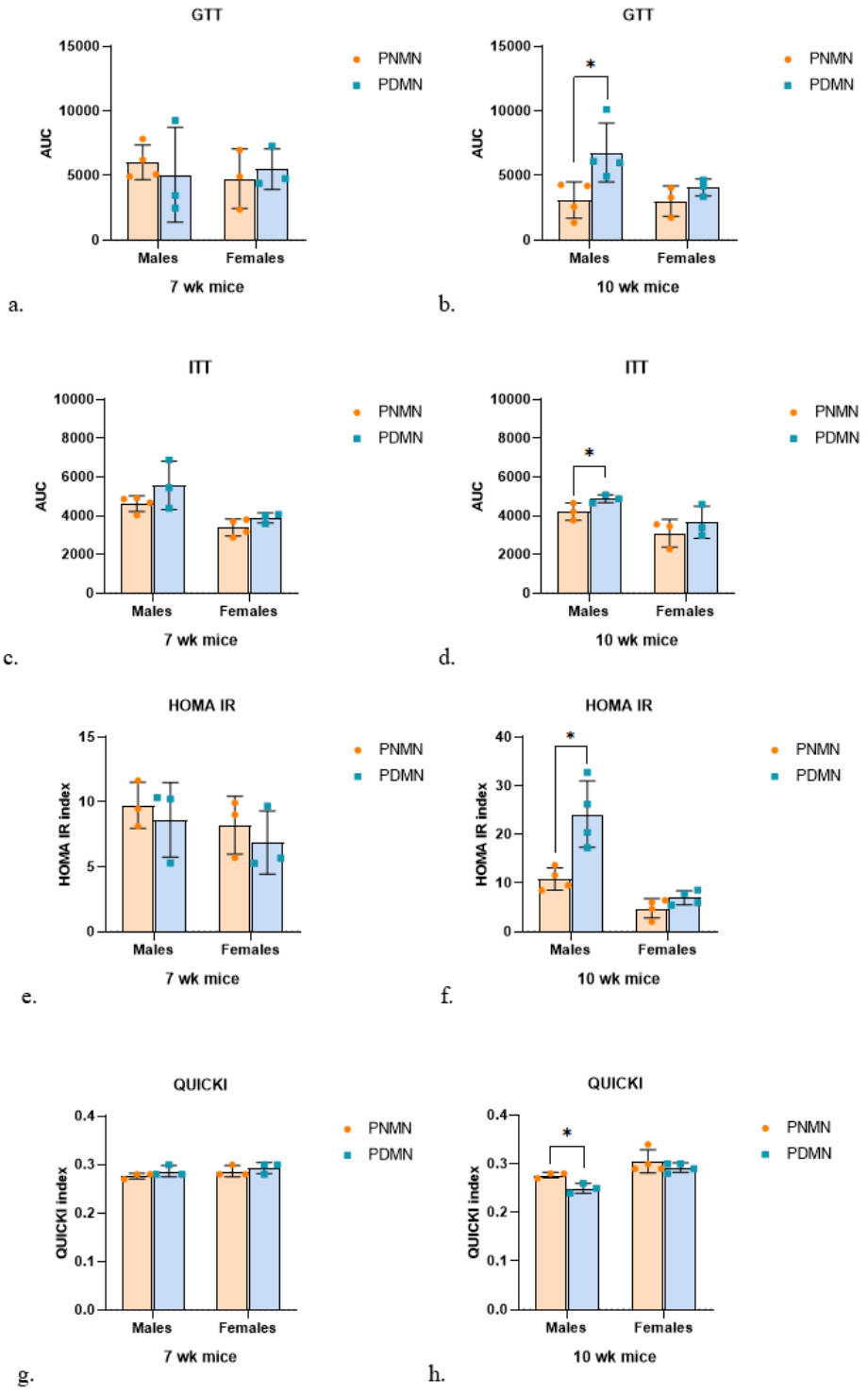


Figure 3

Impact of paternal folate deficiency on insulin sensitivity and glucose tolerance indices. GTT AUC in (a) 7-week mice and in (b) 10-week mice. ITT AUC in (c) 7-week mice and in (d) 10-week mice. HOMA-IR in (e) 7-week mice and in (f) 10-week mice. QUICKI in (g) 7-week mice and in (h) 10-week mice. Data is represented as mean ± SD;PNMN-Paternal normal maternal normal diets, PDMN-Paternal deficient maternal normal diets. *p<0.05 vs. PNMN control.

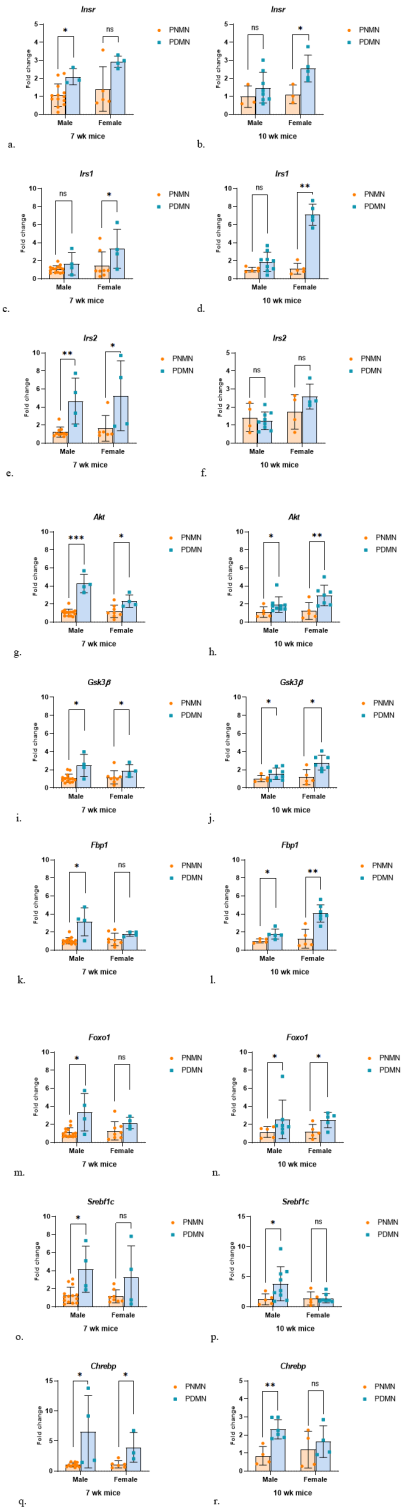


Figure 4

Hepatic mRNA expression of insulin-signaling, gluconeogenic and lipogenic genes. *Insr* expression at (a) 7 weeks and (b) 10 weeks. *Irs1* expression at (c) 7 weeks and (d) 10 weeks. *Irs2* expression at (e) 7 weeks and (f) 10 weeks. *Akt2* expression at (g) 7 weeks and (h) 10 weeks. *Gsk3β*expression at (i) 7 weeks and (j) 10 weeks. *Fbp1* expression at (k) 7 weeks and (l) 10 weeks. *Foxo1* expression at (m) 7 weeks and (n) 10 weeks. *Srebf1c* expression at (o) 7 weeks and (p) 10 weeks. *Chrebp* expression at (q) 7 weeks and (r) 10 weeks. Expression was normalized to β-actin; mean ± SD; *p < 0.05, **p < 0.01, ***p < 0.001 vs. PNMN.

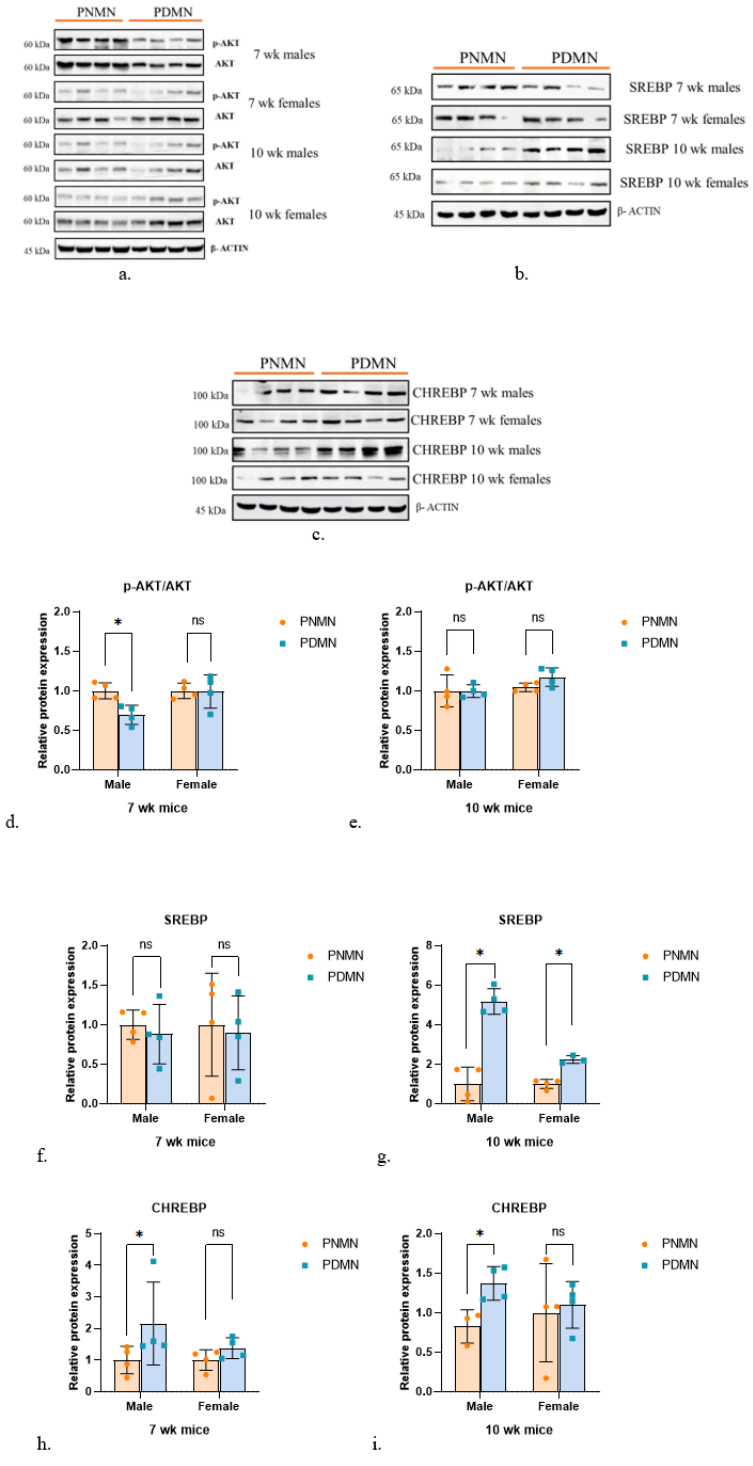
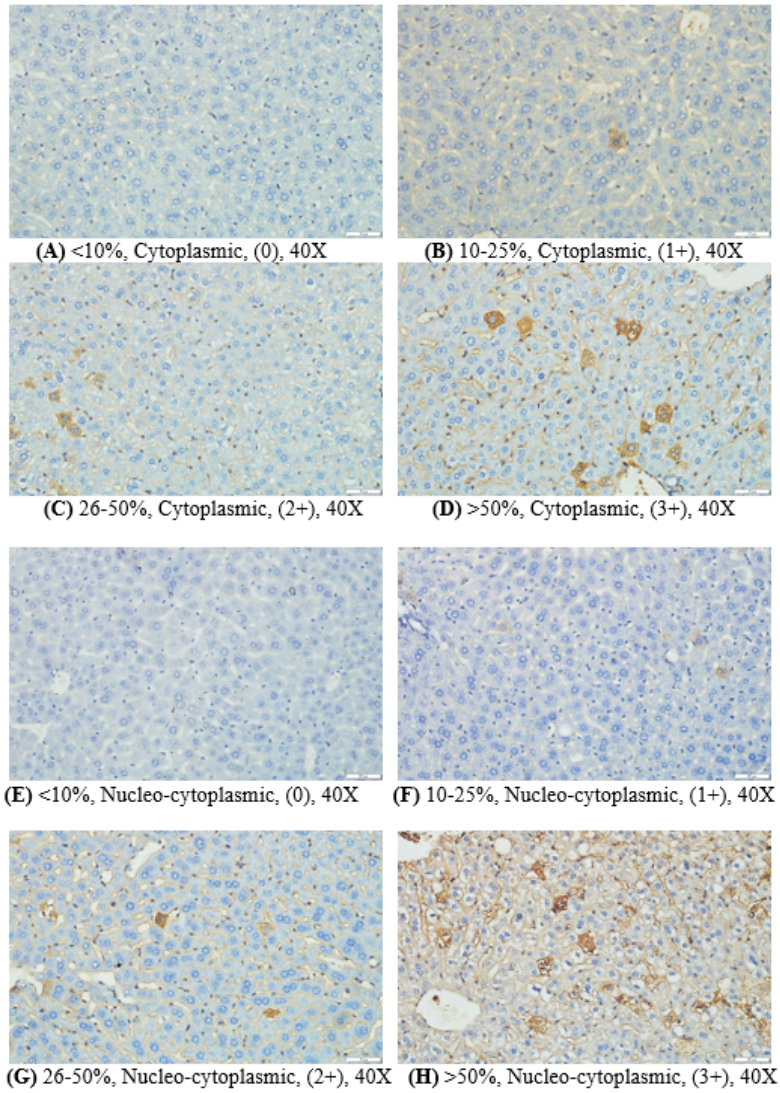


Figure 5

Hepatic protein levels of p-AKT, SREBP-1c and CHREBP. Representative western blots for (a) p-AKT (Ser473), total AKT, (b) SREBP, (c) CHREBP and β-ACTIN in males and females at 7 and 10 weeks. Quantification of p-AKT/AKT ratio at (d) 7 weeks and at (e) 10 weeks. SREBP protein levels in males and females at (f) 7 weeks and at (g) 10 weeks normalized to housekeeping β-ACTIN. CHREBP protein levels in males and females at (h) 7 weeks and at (i) 10 weeks normalized to housekeeping β-ACTIN. Data represented as mean ± SD. *$p<0.05$ vs. PNMN control.



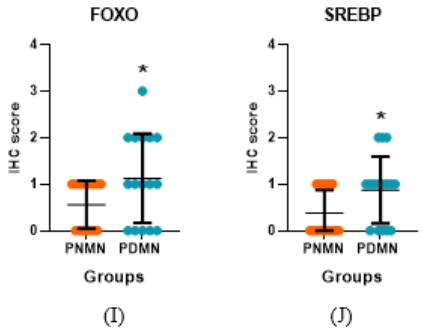


Figure 6

Immunohistochemical analysis of FOXO1 and SREBP-1c in liver. Photomicrographs showing expression and localization of various proteins in liver tissues of PNMN and PDMN mice. Images (40X; scale bar=50μm) were captured using Olympus light microscope (A-D) Cytoplasmic FOXO1 staining intensities: (A) score 0 (<10%), (B) 1+ (10–25%), (C) 2+ (26 50%), (D) 3+ (>50%). (E-H)

Nucleo-cytoplasmic SREBP-1c staining: (E) 0, (F) 1+, (G) 2+, (H) 3+. (I) Cytoplasmic FOXO1 IHC scores; (J) Nucleo-cytoplasmic SREBP-1c scores. Scale bar = 50 μm; mean ± SD; *p < 0.05 vs. PNMN.

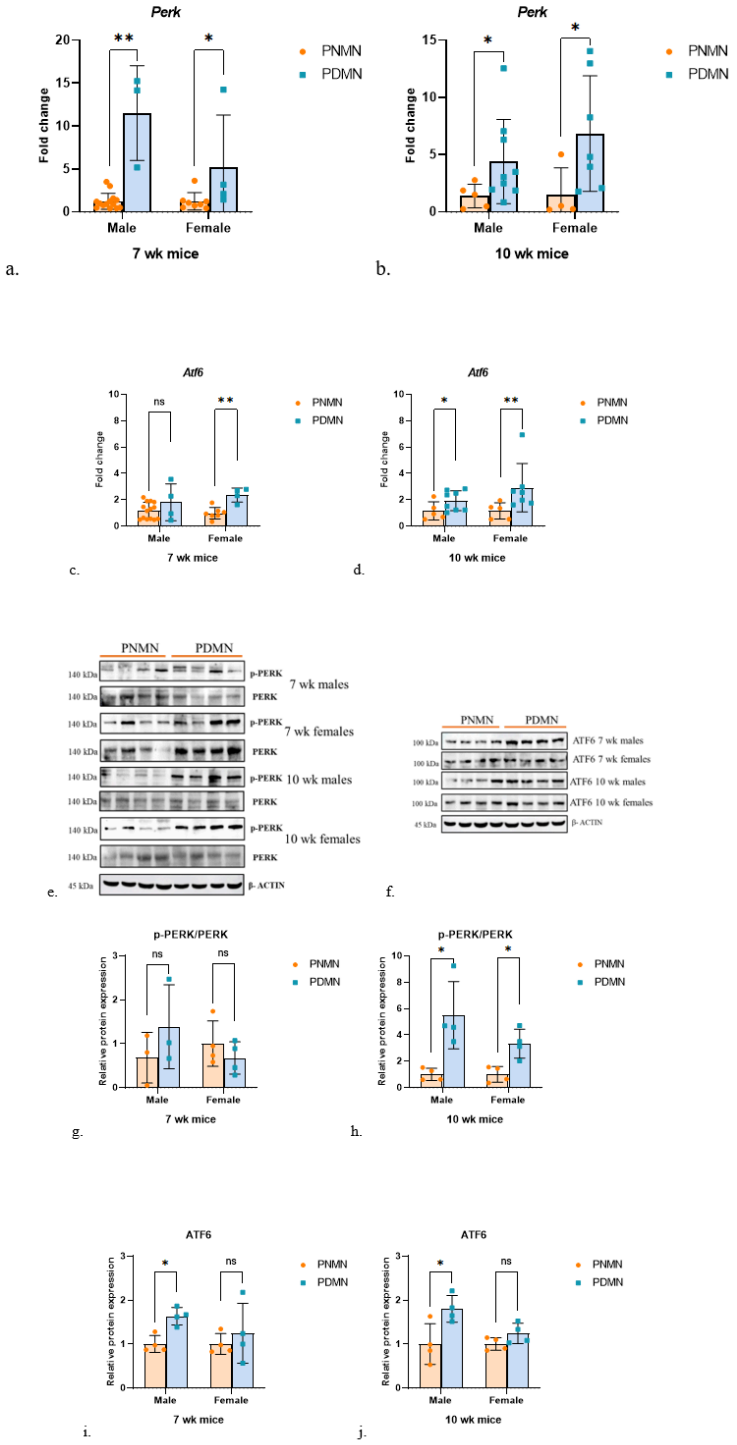


Figure 7

Effect of paternal folate deficiency on ER stress markers Perk and Atf6. mRNA expression levels of *Perk*gene at (a) 7 weeks and (b) at 10 weeks,

expression of *Atf6* gene at (c) 7 weeks and at (d) 10 weeks. Western blot images for (e) p-PERK, total PERK, (f) ATF6 and β-ACTIN in males and females at 7 and 10 weeks. Quantification of p-PERK/PERK at (g) 7 weeks and at (h) 10 weeks. CHREBP protein levels in males and females at (i) 7 weeks and at (j) 10 weeks normalized to housekeeping β-ACTIN. Data represented as mean ± SD. *p<0.05 vs. PNMN control.

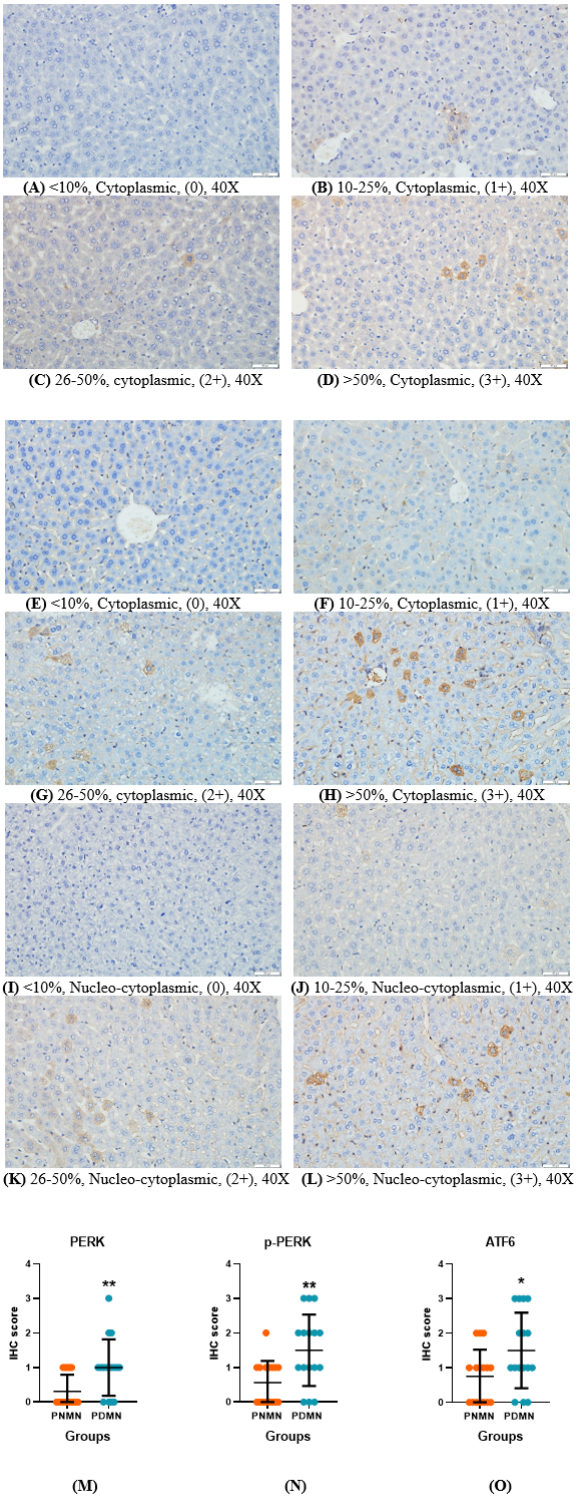


Figure 8

Immunohistochemical analysis of PERK, p-PERK and ATF6 in liver. Photomicrographs showing expression and localization of various proteins in liver tissues of PNMN and PDMN mice. Images (40X; scale bar=50μm) were captured using Olympus light microscope (A–D) Cytoplasmic PERK staining intensities: (A) score 0 (<10%), (B) 1+ (10–25%), (C) 2+ (26 50%), (D) 3+ (>50%). (E–H) Cytoplasmic p-PERK staining: (E) 0, (F) 1+, (G) 2+, (H) 3+. (I–L) Nucleo-cytoplasmic ATF6 staining: (I) 0, (J) 1+, (K) 2+, (L) 3+. (M) Cytoplasmic PERK IHC scores; (N) Cytoplasmic p-PERK scores; (O) Nucleo-cytoplasmic ATF6 scores. Scale bar = 50 μm; mean ± SD; *p < 0.05, **p < 0.01 vs. PNMN.

Supplementary Files

This is a list of supplementary files associated with this preprint. Click to download.

- Supplementaryfig.1.pdf
- Supplementaryfig.2.pdf